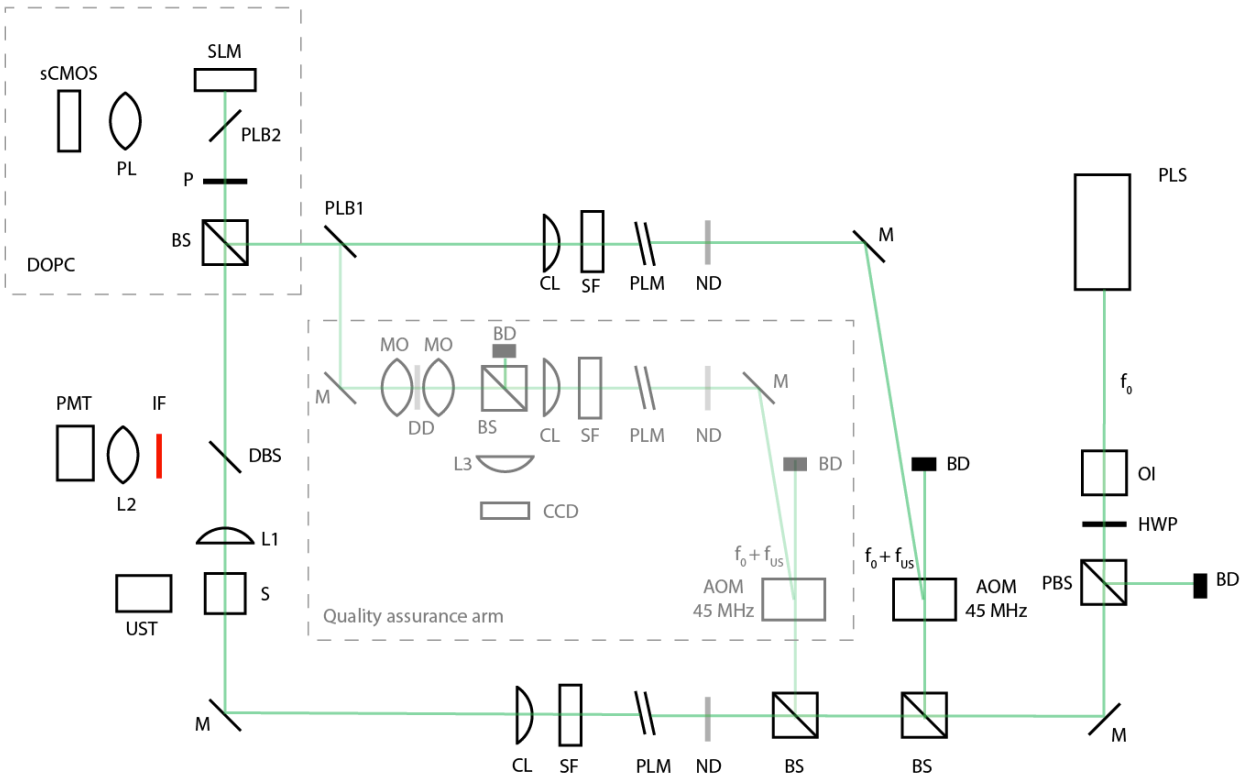

Supplementary Figure 1 | Setup diagram: Abbreviations: Pulsed laser source (PLS), Optical Isolator (OI), Half-wave plate (HWP), Polarizing beamsplitter (PBS), Beam dump (BD), Mirror (M), 50/50 cube beamsplitter (BS), Acousto-optic modulator (AOM), Neutral density filter-wheel (ND), Path length matching arm (PLM), Single-mode fiber acting as spatial filter (SF), Collimating lens (CL), Sample (S), Ultrasound transducer (UST), 50 mm planoconvex lens (L1), Dichroic beamsplitter (DBS), Interference filter (IF), 25 mm planoconvex lens (L2), Photomultiplier tube (PMT), Polarizer (P), 90/10 plate beamsplitter (PLB1), Digital optical phase conjugation setup (DOPC), 50/50 plate beamsplitter (PLB2), Photography compound lens (PL), sCMOS camera (sCMOS), Spatial light modulator (SLM), 300 mm plano-convex lens (L3), Microscope objective (MO), Diffuser disk (DD).

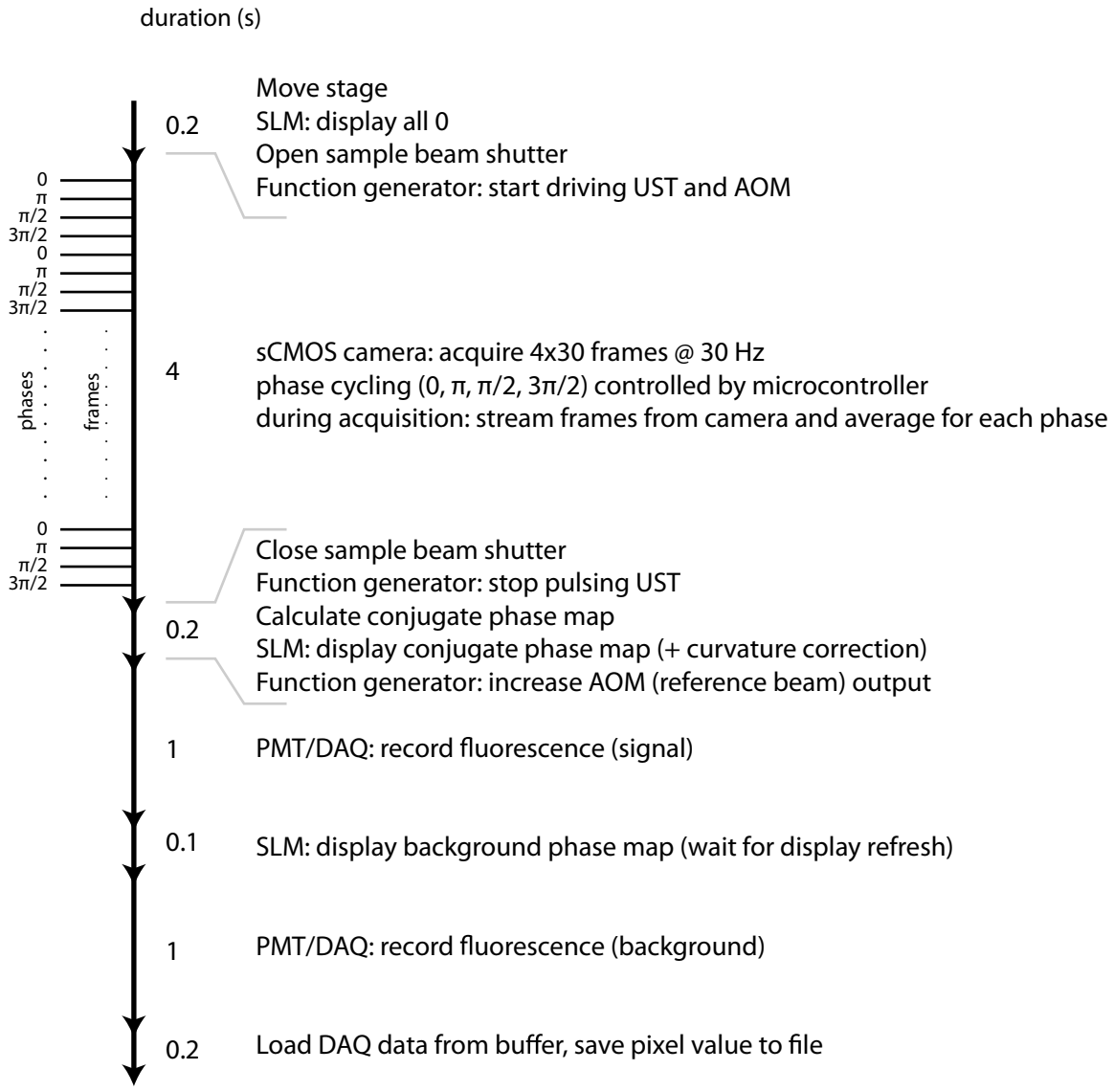

Supplementary Figure 2 | Timing of acquisition: Abbreviations: Spatial light modulator (SLM), Ultrasound Transducer in sample beam path (UST), Acousto-optic modulator in reference beam path (AOM), Photomultiplier (PMT), Data acquisition device (DAQ). For sequential camera exposures (from frame to frame), the phase is cycled between 0, π, π/2 and 3π/2. Frames corresponding to each respective phase are averaged. The averaged data for each phase shift is used for the calculation of the phase maps. The total duration for acquisition of each data point is 6.7 s.

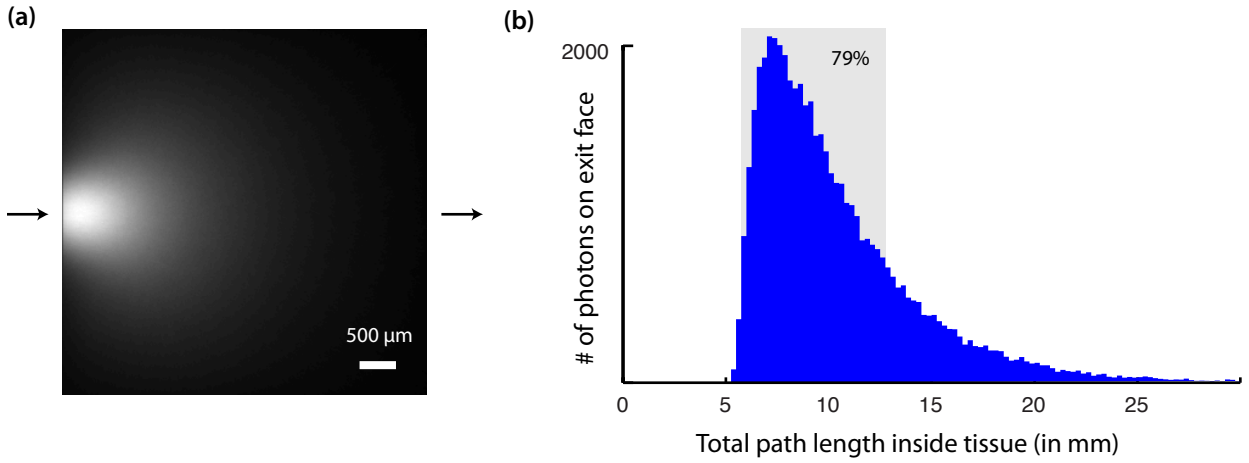

Supplementary Figure 3 | Effects of coherence length: Only those scattered photons whose path lengths have not spread beyond the laser coherence length (in our case: 7 mm) will be detected by the phase-shifting holography scheme. To confirm that most of the scattered photons fall within this window, we ran a single layer Monte Carlo simulation of photon transport [53], where a 0.8 mm wide (FWHM) collimated gaussian beam was incident on a $(5\ \text{mm})^3$ cube of tissue, mimicking the two 2.5 mm thick slabs in our experiments (μ_s = 30/mm, g = 0.965). We launched 10^6 photons in this simulation. (a) shows a 2D projection of the normalized photon flux. The path length distribution of the photons leaving the exit face is plotted in (b). We find that 79% of the scattered photons fall within a 7 mm window, thus confirming that the majority of the photons will be detected and time-reversed. Scale bar: 500 µm

SUPPLEMENTARY METHODS

Description of complete time-reversal

We represent the ultrasound-modulated speckles in the plane of the US focus (A) by the electric field E_A. Upon further propagation through scattering tissue and free space, the ultrasound-modulated field at the detection plane (B) is

$$E_A = T_{AB} E_A \quad \text{S1}$$

where T_{AB} is the complete transmission matrix (with complex transmission values) describing the propagation of E_A from the plane containing the US focus (A) to the detection plane (B). In the case of perfect phase conjugation, where the full solid angle of the scattered wavefront is intercepted and time-reversed, T_{AB} is unitary, lossless and time-symmetric. Thus, the phase-conjugated field back at plane A, E_A', is described by

$$E_A' = T_{BA}(T_{AB} E_A)^* = T_{BA} T_{BA}^{\dagger} E_A^* = E_A^* \quad \text{S2}$$

recovering the ultrasound-modulated field at plane A (where $*$ denotes complex conjugate and † denotes the complex transpose of a matrix). Therefore, theoretically, the electric field of the speckles in the ultrasound focus can be faithfully reconstructed without error when the scattered field is completely time-reversed.

Derivation of peak-to-background ratio in partial phase conjugation

Because of the finite etendue of real phase-conjugate mirrors, only a fraction of the scattered wavefront intercepted is time-reversed. As a result, the transmission matrix is no longer unitary. In a random scattering medium, the transmission matrix can instead be approximated by a random matrix with elements independently drawn from a circular complex Gaussian distribution, with $\mu = 0$ and $\sigma_{real} = \sigma_{complex} = \sigma$ [37]. Using the framework of Vellekoop [37],

we show that a background always exists in the case of partial phase conjugation. Furthermore, the expected ratio of the peak intensity of the phase conjugate focus and its background can be found. We consider two cases – phase and amplitude time reversal and phase only time reversal. The former is relevant to the general case of phase conjugation using photorefractive crystals and digital phase conjugate mirrors with phase and amplitude controls; the latter is specific for our system where only the phase of the scattered field is time-reversed.

In both cases, we describe M input channels (speckles) in the ultrasound focus at plane A as a vector with elements, $\hat{E}_m^A$. We let t_{mn}^{AB} be the complex elements of the transmission matrix mapping each of the M input channels (speckles) to the N possible output modes intercepted by the finite area phase conjugate mirror at plane B, where the output channels are represented by the a vector with elements $\hat{E}_n^B$. We consider first a system with only one non-zero input mode (corresponding to a single-mode source). Without the loss of generality, we let this non-zero input mode be $\hat{E}_1^A$. Thus, we obtain

$$\hat{E}_n^B = \sum_m^M t_{mn}^{AB} \hat{E}_m^A = t_{1n}^{AB} \hat{E}_1^A \tag{S3}$$

Case 1: Phase and amplitude time-reversal

Assuming the phase conjugate mirror has unit reflectivity and invoking the time-symmetric property of the transmission matrix, the phase conjugate, $\hat{E}_1^{A'}$ is

$$\hat{E}_1^{A'} = \sum_n^N t_{1n}^{BA} \left(t_{n1}^{AB} \hat{E}_1^A\right)^* = \left(\hat{E}_1^A\right)^* \sum_n^N |t_{1n}^{AB}|^2 \tag{S4}$$

and its intensity is

$$\hat{I}_1^{A'} = \left[\left|\hat{E}_1^A\right| \sum_n^N |t_{1n}^{AB}|^2\right]^2 = \hat{I}_1^A \left[\sum_n^N |t_{1n}^{AB}|^2\right]^2 = \hat{I}_1^A \alpha^2 \quad \text{S5}$$

Thus, we find that the input speckle considered is reconstructed with some pre-factor, $\alpha^2 = [\sum_n^N |t_{1n}^{AB}|^2]^2$, determined by the transmission properties of the turbid medium. In a random scattering medium, the ensemble average of α^2 can be found by considering the statistics of the circular Gaussian distribution and in so recognizing that α itself follows the Gamma distribution, $\Gamma(N, 2\sigma^2)$. We thus obtain

$$\langle \alpha^2 \rangle = 4N(N+1)\sigma^4 \quad \text{S6}$$

We will now show that the elements at plane A with zero input will have non-zero phase conjugate intensities (i.e. $\hat{I}_m^{A'} > 0 \; for \; m \neq 1$), constituting a phase conjugate background. We let the transmission through channel n at plane B back to any input mode $m \neq 1$ at plane A be $t_{nm\neq 1}^{BA}$. Upon playback of the phase conjugate field for $\hat{E}_1^{A'}$, the intensity at plane A where $m \neq 1$ is

$$I_m^{A'} = \hat{I}_1^A \left|\sum_n^N t_{n1}^{AB} t_{nm}^{BA}\right|^2 = \hat{I}_1^A \beta^2, \qquad for \; m \neq 1 \quad \text{S7}$$

where the ensemble average of $\beta^2 = |\sum_n^N t_{n1}^{AB} t_{nm\neq 1}^{BA}|^2$ can be found using the statistics of a complex circular Double Gaussian distribution:

$$\langle \beta^2 \rangle = \langle \left|\sum_n^N t_{n1}^{AB} t_{nm}^{BA}\right|^2 \rangle = 4N\sigma^4, \qquad for \; m \neq 1 \quad \text{S8}$$

It is clear then that there is a non-zero average background intensity associated with the phase-conjugated speckle, and that the ratio of that phase-conjugated speckle to its background is:

$$\frac{\langle \alpha^2 \rangle}{\langle \beta^2 \rangle} = N + 1 \quad \text{S9}$$

When there are M non-zero inputs, this result is scaled by M [37], such that the focal peak-to-background ratio (*PBR*) is

$$PBR_{phase\ \&\ amplitude} = \frac{\langle I'_m \rangle}{\langle I'_o \rangle} = \frac{N+1}{M} \tag{S10}$$

Experimentally, N is related to the number of uncorrelated speckles intercepted by the phase conjugate mirror and its upper limit is determined by the number of pixels on the spatial light modulator; M is the number of speckles modulated by the ultrasound and thus decreases as the ultrasound focus decreases.

Case 2: Phase only time-reversal

In the case where a phase only phase conjugate mirror is used, the phase-conjugated electric field and intensity of the input speckle, respectively, are

$$\hat{E}_1^{A\prime} = \left(\hat{E}_1^A\right)^* \sum_n^N t_{1n}^{BA} \exp\left[-i \cdot Arg(t_{n1}^{AB})\right] = \sum_n^N |t_{1n}^{BA}| \tag{S11}$$

$$\hat{I}_1^{A\prime} = \hat{I}_1^A \left[\sum_n^N |t_{1n}^{BA}|\right]^2 \tag{S12}$$

and the derivations of $PBR_{phase\ only}$ follows exactly that of [37] for the case of iterative wavefront optimization to multiple targets through scattering medium, obtaining for $N \gg 1$:

$$PBR_{phase\ only} = \frac{\pi}{4}\frac{(N-1)+1}{M} \approx \frac{\pi}{4} \cdot PBR_{phase\ \&\ amplitude} \tag{S13}$$

Phase jitter in acoustic wave

Our technique relies on the detection of 45 MHz ultrasound frequency-shifted light in the presence of a large background of non-shifted light. While the reference beam (equally frequency-shifted by 45 MHz) interferes with US-tagged light, interference of the reference beam with the non-shifted light occurs at a beating frequency of 45 MHz (cycle time: 22.2 ns). This beating usually averages out during the much longer integration time of the CMOS camera. But if the illumination is pulsed, the pulse duration approaches one beating cycle or less and the phase of the beating is locked to the laser trigger output, the interference between the non-shifted beam and the shifted beam may nevertheless be detected. This would not be desirable in our case, since a small phase drift between the non-shifted beam and the reference beam would lead to an added artificial signal on the phase map we measure. To ensure that such coherent effects between the non-shifted beam and the frequency-shifted beam are not detected on our camera, we randomly alternate between two trigger delays of a time difference that corresponds to half a 45 MHz beating cycle (11.1 ns or $\pm$ 5.5 ns). A microcontroller randomly chooses a jitter for each laser sync output pulse (at a rate of 20 kHz) and the jitter is added to the trigger delay of ultrasound transducer as well as reference beam AOM. The relative phase between ultrasound-shifted light and the reference beam therefore remains unaffected.

SUPPLEMENTARY REFERENCE

[53] Wang LV and Wu H, "Biomedical Optics: Principles and Imaging." Wiley 2007